Cooperative Heterometallic Catalysts for Lactide Ring-Opening Polymerization: Combining Aluminum with Divalent Metals

Cooperative Heterometallic Catalysts for Lactide Ring-Opening Polymerisation: Combining Aluminium with Divalent Metals

*Anand J. Gaston, Zoe Greindl, Carole A. Morrison, Jennifer A. Garden**

EaStCHEM School of Chemistry, University of Edinburgh, EH9 3FJ, UK

KEYWORDS: poly(lactic acid) heterometallic catalysis aluminum salen

While homometallic (salen)Al catalysts display excellent performance in lactide ring-opening polymerisation (ROP), heterometallic (salen)Al complexes have yet to be reported. Herein, we describe four heterobimetallic (salen)Al catalysts, and show that the choice of the heterometal is key. Cooperative Al/Mg and Al/Zn combinations improved the catalyst activity by a factor of up to 11 compared to the mono-Al analogue, whereas the mono-Mg and mono-Zn analogues were completely inactive. In contrast, Al/Li and Al/Ca heterocombinations stunted the polymerisation rate. Kinetic and computational studies suggest that Al/Mg and Al/Zn cooperativity arises from the close intermetallic proximity facilitating chloride bridging (thus enhancing initiation), which promotes a rigid square pyramidal geometry around the Al centre and further increases the available monomer coordination sites. This work also translates the use of ab initio molecular dynamics calculations to ROP, introducing a useful method of investigating catalyst flexibility and

revealing that ligand strain and molecular rigidity can enhance heterometallic catalyst performance.

Introduction

Heterometallic (mixed-metal) cooperativity is an emerging means of improving catalyst activity in small and macro-molecular transformations, and many heterometallic catalysts significantly outperform the monometallic analogues in terms of activity and selectivity.[1] This concept has been well-established in C-H activation,[2] metal-halogen exchange,[3] and olefin polymerisation[4,5] and has shown good promise in ring opening copolymerisation.[6,7] However, within the ring-opening polymerisation (ROP) of cyclic esters, the vast majority of catalyst development has focused on tailored ligand design. Heterometallic reactivity enhancement is an equally promising yet much less explored method of improving ROP catalyst performance, and many of the overarching design principles are still not well understood.[8,9–11]

Poly(lactic acid) (PLA) is a promising degradable alternative to some conventional engineering polymers, with applications ranging from commodity plastics to biomedicine.[12–16] While many monometallic ROP catalysts have been reported, aluminium salen catalysts are particularly notable as they provide excellent stereocontrol,[17–22] yet often suffer from low activity and thus require high temperatures or long reaction times to achieve high conversions. Aluminium salen complexes have been exploited in a range of transformations,[23] including cyclic carbonate synthesis,[24] epoxide resolution,[25] photoredox catalysis,[26] and polycarbonate synthesis,[27] and the salen ligand flexibility has been identified as a key factor in improving the catalyst activity.[17,28,29] On the basis of experimental and computational modelling studies, conventional wisdom in cyclic ester ROP suggests that increasing the length (and therefore the flexibility) of the diamino bridge increases the catalyst activity by enabling access to key transition states. This concept can be further explored

using ab initio molecular dynamics (AIMD), which offer a route to capturing the time-averaged geometry, thus giving a more quantifiable insight into the importance of dynamic atomic movements around the catalytic active site, applicable to a variety of transformations.

Homobimetallic catalysts are often highly active and can outperform the monometallic analogues in cyclic ester ROP,[30–33] with some bis-Al catalysts displaying activities eight times higher than the monometallic analogues, attributed to a proposed bimetallic mechanism (Figure 1).[34,35] Heterobimetallic complexes can further increase polymerisation activity, as electronic communication between the two metals can simultaneously alter the metal Lewis acidity and metal-R bond polarity hence nucleophilicity (where R is alkyl, alkoxy, carbonate or halide).[36,37] To the best of our knowledge only three LA ROP studies have reported heterometallic reactivity enhancements with salen complexes (Ni/La and Cu/Nd), none containing Al.[38–40] Indeed, very few heterobimetallic Al complexes have been reported for LA ROP (based on Li, Na or K/Al, Sm/Al and Y/Al),[41–43] and these have not always led to activity enhancements. Developing new heterometallic aluminium salen complexes not only offers a novel method of improving catalyst activity within LA ROP (as well as other catalytic transformations) but also an opportunity to understand which catalyst features are important in exploiting heterometallic cooperativity.

Heterometallic cooperativity between earth abundant and biocompatible metals is a particularly attractive goal.[44,45] In LA ROP, some of the most active systems are homobimetallic complexes based on magnesium and zinc,[31,46–49] and designing heterometallic complexes offers a route to combine the high activity of Mg or Zn with the control of (salen)Al systems. Herein we report four heterobimetallic complexes supported by an asymmetric salen ligand and reveal the influence of different heterometallic combinations on the structure and catalyst performance.

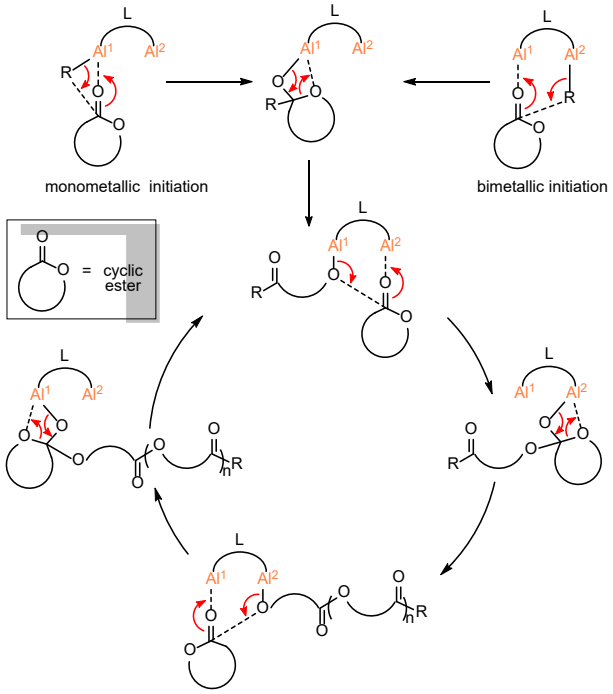

Figure 1 Proposed chain shuttling mechanism for cyclic ester ROP initiated by homobimetallic Al complexes (L = piperazidine-bridged bis(phenolato) / alkyl bridged salen ligand).[34,35]

Results and Discussion

The acid-functionalised salen ligand, **L1** (Figure 2, Figure S1), can be tetra-deprotonated and contains two distinct metallation sites (imine-phenol, N_2O_2; phenol-acid pocket O_2O_2). While both trivalent (Al) and divalent metals (Mg and Zn) were successfully incorporated into the ligand scaffold to form monometallic complexes, the location depended on the metal valency, hardness and electropositivity (refer to ESI for details).

Di-deprotonation of **L1** with Et_2AlCl (Figure 2) gives Al coordination in the O_2O_2 binding pocket. The ^{1}H NMR resonance of the phenolic protons (12.36 ppm in d_6-DMSO, Figure S3) is in a similar range to both phenolic and iminium protons in comparable complexes,[50,51] perhaps indicating a bridged or transient proton state. Conservation of these protons is further evidenced

through unchanged integration and coupling to both imine and backbone proton resonances (Figure S15). Preferential deprotonation and metal coordination within the O_2O_2 pocket can be rationalised by the relative acidity of the carboxylic acid protons ($pK_a \approx 3.0$) *versus* the phenol protons ($pK_a \approx 13.6$) of salicylic acid.[52] Subsequent or simultaneous addition of a second equivalent of Et_2AlCl to **C1** gave no further reaction under the conditions tested. The acidity of the phenolic protons, Brønsted basicity of Et_2AlCl and the well-documented metallation of salen Schiff-base N_2O_2 ligands[29] suggests that bis-metallation with Al may be possible, however the presence of the Al-Cl unit may stabilise the product and lead to electrostatic repulsion or steric hindrance that prevents bis-metallation. This selectivity for mono-metallation of **L1** is a benefit of using Et_2AlCl to prepare heterometallic complexes. While zinc complex **C2** shows exclusive phenol-OH deprotonation, both magnesium isomers (**C3** and **C3'**) were present in a 5:2 ratio (Figures 2, S4-S5). Heating the product mixture in d_6-DMSO changed the **C3**:**C3'** ratio to 10:1, suggesting that proton exchange occurs to give **C3** as the thermodynamic product (Figure S5). The relative metal hardness (Al > Mg > Zn) and metal oxophilicities ($\Theta_{Al} = 0.8 > \Theta_{Mg} = 0.6 > \Theta_{Zn} = 0.2$) reflects the trend for chelation within the O_2O_2 pocket,[53] which contains harder oxygen Lewis donors (*vs* nitrogen).[54] The similar ionic radii of Mg^{2+} (72 pm) and Zn^{2+} (74 pm) suggests that size is not a major factor.[55,56] Rather, the increased conformational flexibility and oxygen bonding afforded by the outer pocket may contribute to the preference for O_2O_2 coordination of Mg and Al (Figure S2).[57–59]

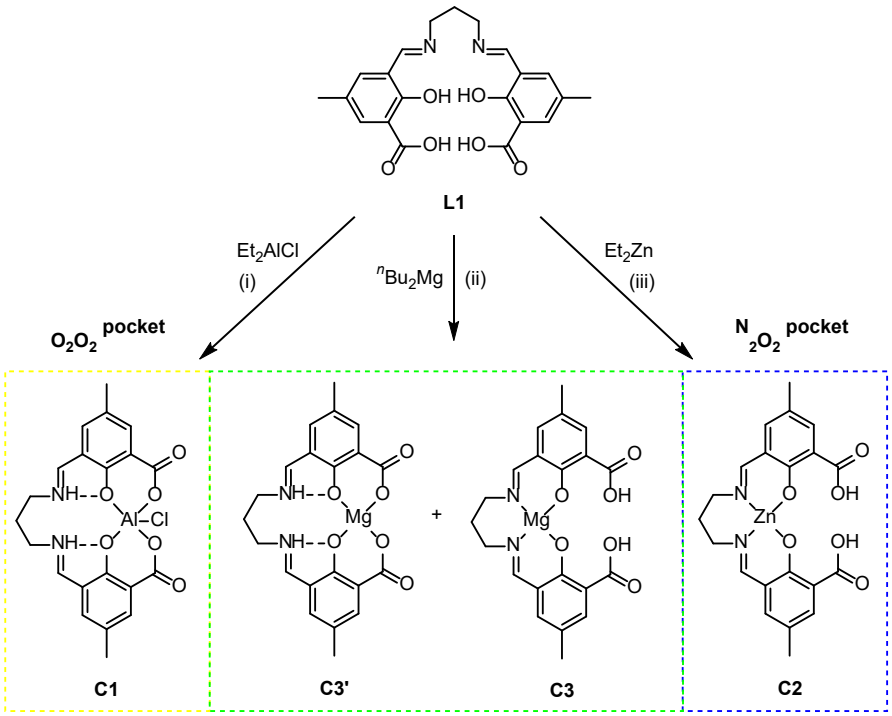

Figure 2 Synthesis of complexes **C1**, **C2** and **C3** highlighting the different metallation sites. Optimised reaction conditions: (i): 1 eq Et_2AlCl in THF at -78 °C; (ii): 1 eq $^nBu_2Mg$ in THF at RT; (iii): 1 eq Et_2Zn in THF at RT.

Most of the heterometallic catalysts reported for LA ROP are based on symmetric ligands,[60] yet asymmetric ligands offer potential benefits in simplifying heterometallic complex synthesis, with distinct binding pockets tailored for different metals (thus helping to avoid mixtures of homo- and hetero-metallic complexes). Heterometallic complexes were selectively obtained by incorporating a second metal (Li, Mg or Ca) into the N_2O_2 binding pocket of **C1** through deprotonation with LiHMDS (**C1a**), $^nBu_2Mg$ (**C1c**) or $CaHMDS_2$ (**C1d**) (Figure 3, iii-v). Direct metallation of **C1** with Et_2Zn generated a mixture of products, and so complex **C1b** was selectively prepared through two alternative routes (Figure 3, vi-vii). Sequential metallation using Et_2Zn then Et_2AlCl (Figure 3, i/vii) was deemed preferable over transmetallation from LiAl complex **C1a** (Figure 3, v/vi), as

this avoided the production of LiCl by-products which were challenging to remove (Figures S47-S48).

With complexes **C1b** (ZnAl) and **C1c** (MgAl), tetra-deprotonation of **L1** was supported by the absence of phenol and carboxylic acid ligand protons, as well as complete reaction of all Zn-Et/Mg-^{n}Bu groups evidenced by ^{1}H NMR spectroscopy (Figure S8). Using 2 equivalents of LiHMDS (**C1a**) or a single equivalent of $CaHMDS_2$ (**C1d**) resulted in the formation of multiple products. Interestingly, reducing the heterometal stoichiometry to 1 or 0.5 equivalents of LiHMDS or $CaHMDS_2$ respectively, gave a single product in the ^{1}H NMR spectrum for each complex (Figures S9 and S10). The absence of phenol protons in these product ^{1}H NMR spectra, despite the reaction stoichiometry, is ascribed to the increased phenol proton acidity and hydrogen bonding/proton fluxionality causing peak broadening. With both **C1a** and **C1d**, incomplete deprotonation of **C1** is likely due to the steric hindrance within the N_2O_2 pocket. The ionic radius of Li^+ (76 pm) is significantly larger than the atomic radius of H (37 pm),[55,56] and whilst it is similar to Mg^{2+} (72 pm) and Zn^{2+} (74 pm), the inclusion of two Li^+ in in the N_2O_2 pocket would greatly increase steric congestion. Similarly, the ionic radius of Ca^{2+} (100 pm) is significantly larger than either magnesium or zinc. Instead of di-deprotonation of **C1** and coordination of calcium in the N_2O_2 pocket, NMR studies suggest that **C1d** comprises two mono-deprotonated **C1** units bridged by calcium. This observation aligns with structural studies on related (salen)Ca and (aminophenol)Ca complexes, where Ca is situated above the ligand plane to reduce steric hindrance around the metal centre enabling coordination to two ligands.[61,62] Complex **C1d** was also analysed using ICP-OES, which confirmed the 2:1 Al:Ca ratio. ^{1}H NMR spectroscopy showed complete loss of the Ca-HMDS ligand resonance at -0.12 ppm, as well as the formation of HMDSH (δ = 0.01 ppm, Figures S10, S37).

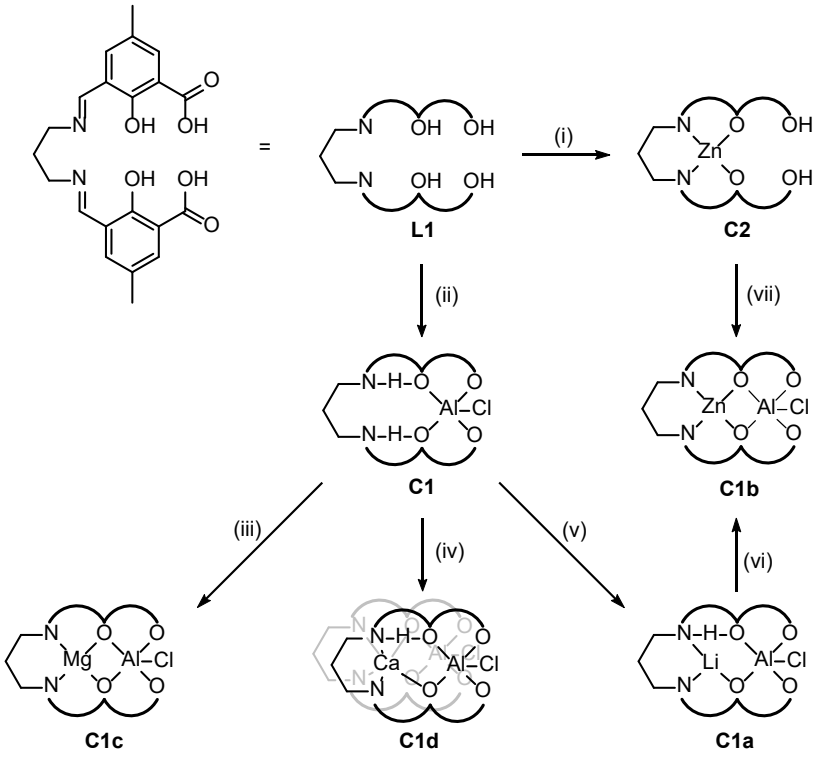

Figure 3 Reactivity scheme for **L1** and complexes **C1**, **C2** and **C1a-d**. Reaction conditions: (i): 1 eq Et_2Zn in THF at -78 °C; (ii): 1 eq Et_2AlCl in THF at -78 °C; (iii): 1 eq $^nBu_2Mg$ in DMSO at RT; (iv): 0.5 eq $CaHMDS_2$ in DMSO at RT; (v): 1 eq LiHMDS in DMSO at RT; (vi): 1 eq $ZnCl_2$ in DMSO at RT; (vii): 1 eq Et_2AlCl in DMSO at RT.

The ^{1}H imine resonances of **C1a-C1d** correlate with the heterometal electropositivity (Figure S8), with an upfield shift relative to monometallic **C1** (δ = 8.81 ppm; **C1b**, 8.43 ppm, χ_{Zn} = 1.65; **C1c**, 8.40 ppm, χ_{Mg} = 1.31; **C1d**, 8.24 ppm, χ_{Ca} = 1.00; **C1a**, 8.20 ppm χ_{Li} = 0.98). Incorporating a heterometal can thus modify the electronics of the complex, akin to the better explored use of electron withdrawing/electron donating ligand substituents to modulate catalyst activity in

ROP.[28,29,63] Unfortunately, crystals of complexes **C1** and **C1a-d** suitable for X-ray diffraction studies could not be obtained due to limited complex solubility.

To explore the structural effect of incorporating a heterometal within the ligand, a series of geometry optimisation calculations were performed for complexes **C1** and **C1a-C1c**, at the B3LYP/6-311G* level (see ESI). In heterobimetallic complexes **C1a-C1c**, DFT simulations support the metal arrangement predicted by ^{1}H NMR analysis, with Al in the O_2O_2 binding pocket and Li/Zn/Mg within the N_2O_2 pocket (form I, Table 1). Conversely, DFT models of homometallic **C1** determined the lower energy conformation is form II, albeit with a difference of just 9.2 kJ mol^{-1} (Table S2). These calculations suggest that the **C1-I** (form I) structure observed experimentally is likely to be the kinetic, rather than the thermodynamic, metallation product. The low energy difference between **C1-I** and **C1-II** indicates that experimental conditions and solvent effects may influence the product distribution. The geometry around Al was investigated to determine the τ5 character (where 0.00 represents an ideal square pyramidal geometry and 1.00 represents an ideal trigonal bipyramidal geometry).[64] For each complex, form I displayed greater square pyramidal character and a reduced inter-metal separation (by c.a. 0.1 – 0.4 Å, Table 1). For all heterometallic complexes, the Cl atom resides closer to the heterometal in form I (*vs* form II), as demonstrated by shorter M-Cl distances and increased Al-Cl bond lengths (Table 1). The short M-Cl distances observed for **C1a** and **C1c** suggest a μ^2-Cl binding motif.

Table 1 Top: Structural comparison of form I and form II of complexes **C1** (X = H), **C1a** (X = Li), **C1b** (M = Zn) and **C1c** (M = Mg). Bottom: Comparison of Al metal geometry, internal strain, intermetallic separation and Al-Cl bond length of complexes **C1** and **C1a**-**C1c**, calculated at the B3LYP/6-311G* level.

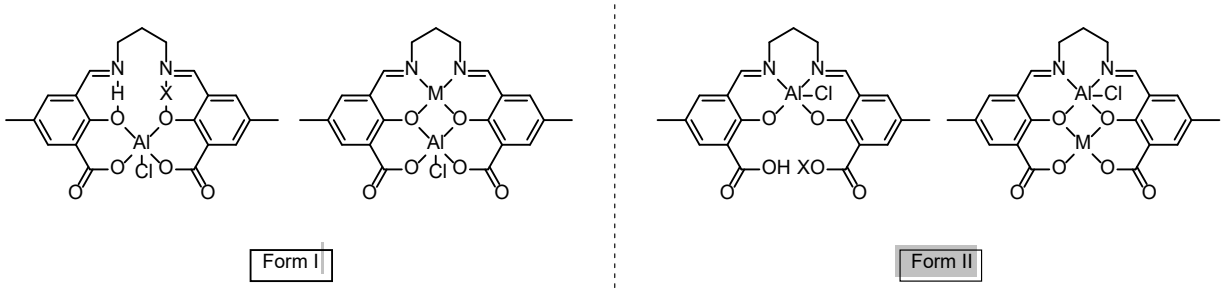

Complex	τ5 character[a]	ΔG_{strain} (kJ mol^{-1})	Intermetallic separation (Å)	Al – Cl bond length (Å)	M – Cl bond length / distance (Å)
C1-I	0.71	82.5	-	2.20	-
C1-II	0.87	120.4	-	2.18	-
C1a-I	0.57	159.9	2.93	2.27	2.32
C1a-II	0.83	152.1	3.32	2.17	4.20
C1b-I	0.15	188.0	3.04	2.20	3.46
C1b-II	0.53	166.5	3.14	2.17	4.23
C1c-I	< 0.01	197.2	2.83	2.32	2.60
C1c-II	0.54	170.2	3.08	2.17	4.13

[a] τ5 character determined according to the method published by Addison, Reedijk *et al*.[64]

To investigate the structure and dynamics of **C1-I** and **C1a**-**C1c-I** in more detail, AIMD simulations were performed to calculate the thermal motion of all atoms at room temperature over a 6 ps timescale (see ESI).[65,66] The resulting time averaged structures (Figure 4), with atomic displacement parameters (ADPs) expressed at the crystallographic standard 50% probability

ellipsoidal level, capture significant functional group movement and provide insight into the structure-activity trends expressed by these complexes. Complex **C1** has a high degree of structural mobility, which is particularly noticeable at the chloride and aromatic carbon centres. Multiple proton transfer events were observed along the N…H…O hydrogen bond linkage in the N_2O_2 pocket, resulting in the bridging time-averaged ellipsoidal model shown in Figure 4. Incorporating a heterometal increases the rigidity through the formation of additional six-membered ring(s), with MgAl complex **C1c** displaying the highest rigidity of all (Figure 4). All three heterobimetallic structures show a bridging Cl-heterometal interaction. The identity of the heterometal appears to directly affect the Cl mobility: the small Cl ADP observed in rigid **C1c** contrasts markedly with the larger ADP of the ZnAl **C1b** structure, which suggests a high degree of flux between a bridged and non-bridged state in **C1b**. This increased flux in **C1b** (*vs* **C1a** and **C1c**) is likely due to the Lewis acidity of the heterometal, with shorter M-Cl distances observed for the most electropositive metals (χ_{Li} = 0.98, M-Cl = 2.30 Å; χ_{Mg} = 1.31, M-Cl = 2.63 Å; χ_{Zn} = 1.65, M-Cl = 2.80 Å). The increased Al-Cl bond length in complexes **C1a** (2.28 Å), **C1b** (2.22 Å) and **C1c** (2.30 Å) relative to monometallic **C1** (2.03 Å) is attributed to the dative M-Cl bond lengthening, thereby weakening the Al-Cl bond.

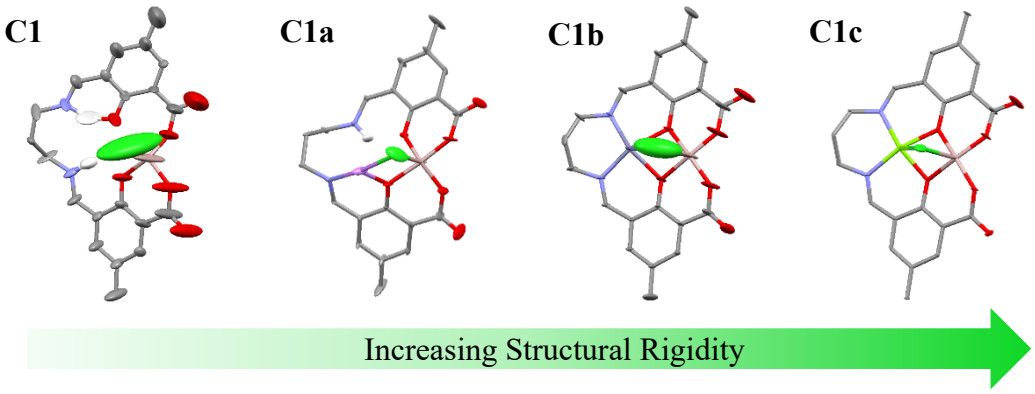

Figure 4 AIMD time-averaged structures of complexes **C1** (left), **C1a** (middle left), **C1b** (middle right) and **C1c** (right).

Complexes **C1-3** and **C1a-C1d** were tested for their activity toward *rac*-lactide (*rac*-LA) ROP. The complex, initiator (propylene oxide, PO) and monomer (*rac*-LA) were mixed in a 1:50:100 ratio in toluene at 120 °C, conditions chosen as optimised for homometallic (salen)AlCl initiators (Table 2, Table S1 and Figure 5).[28] The polymerisation was also tested with a 1:1 catalyst:PO ratio, however this significantly reduced the catalyst activity, likely due to inefficient initiation reflected by higher than predicted M_n values (Table S1, entry 20). In line with previously reported (salen)AlCl complexes, monometallic **C1** was inactive towards *rac*-LA ROP; however, *in situ* ring-opening of PO generated an active aluminium alkoxide initiator (Table S1, entries 1-6). Complexes **C1b** (ZnAl, k_{obs} = 1.8 x 10^{-3} s^{-1}) and **C1c** (MgAl, k_{obs} = 8.8 x 10^{-3} s^{-1}) both displayed marked reactivity enhancements, outperforming homometallic **C1** by respective factors of 2 and 11 (Al, k_{obs} = 0.8 x 10^{-3} s^{-1}, Figure 5) and forming atactic PLA. MALDI-ToF end-group analysis confirmed initiation *via* PO ring-opening (Figure S57). Both complexes **C1b** and **C1c** produced PLA with a similar degree of control to monometallic **C1** (Đ ≈ 1.2). PLA with increased dispersity and poor M_n agreement was obtained at high conversions using **C1b** (Table 2, entry 8, Đ = 1.63), which is attributed to post polymerisation transesterification reactions such as the formation of cyclic PLA as evidenced by MALDI-ToF analysis (Figure S58). It is also possible that the zinc complex may catalyse some depolymerisation in the late stages of the reaction, as has been reported for some other zinc-based catalysts.[67,68] **C1b** was also tested with higher lactide loading (300-1000 eq, Table S1 entries 21-23) displaying good activity and similar polymerisation control, albeit with a slight reduction in catalyst activity. In contrast to **C1b**, **C1c** yields good M_n agreement; the improved propagation rate of catalyst **C1c** may outcompete transesterification to give greater control over the resultant PLA.

Table 2 *Rac*-lactide ROP mediated by catalysts **C1** and **C1a-C1d**.[a]

Entry	Catalyst	Time (min)	% Conversion[b]	$M_{n,calc}$ / Da[c]	$M_{n,obs}$ / Da[d]	Đ[d]
1[e]		30	-	-	-	-
2	**C1**	5	9	1270	810	1.25
3		10	24	3490	2710	1.10
4		40	83	11910	7640	1.21
5	**C1a**	5	3	400	390	1.02
6		30	24	3490	1600	1.35
7	**C1b**	5	6	900	670	1.10
8		30	94	13500	5610	1.63
9	**C1c**	2	48	6980	7190	1.14
10		5	80	11550	8930	1.22
11		10	90	13020	10140	1.25
12	**C1d**	5	3	-	-	-
13		15	7	-	-	-
14	**C2**	30	-	-	-	-
15	**C3**	30	-	-	-	-

[a] Reaction conditions: 0.0212 mmol catalyst [catalyst]/[PO]/[*rac*-LA] = 1:50:100, [*rac*-LA] = 1 M in toluene, 120 °C. [b] Determined by ^{1}H NMR spectroscopy. [c] Calculated as ([*rac*-LA]/[catalyst])×(%conversion/100)×MW of lactide, assuming that only one chain grows per catalyst system. [d] Determined by size-exclusion chromatography (SEC) in THF, universal calibration relative to polystyrene standards, M_n was calculated considering Mark–Houwink's corrections for M_n (M_n(calc) = 0.58[M_n(SEC)]).[73] [e] No PO added.

Previously reported Al-salen catalysts have been tested under a range of conditions, with reported k_{obs} values typically ranging from 1.9 x 10^{-6} to 6.9 x 10^{-3} s^{-1}.[19,20,28,35,63,69–72] While the different conditions limit direct comparison, to the best of our knowledge the incorporation of Mg within complex **C1c** gives the fastest (salen)Al-chloride catalyst reported for *rac*-LA ROP to date (k_{obs} = 8.8 x 10^{-3} s^{-1}, Figures S55 and S56). While these heterometallic (salen)Al catalysts are

slower than the fastest homometallic Mg and Zn catalysts for *rac*-lactide ROP, they display good activities compared to state-of-the-art Al systems albeit under different reaction conditions (Figure S64, Table S4), and provide insight into the features underpinning heterometallic cooperativity.

The reactivity enhancement observed with complexes **C1b** and **C1c** is partly attributed to the presence of the second, Lewis acidic metal providing additional monomer coordination sites. The cooperative bimetallic mechanism proposed by Yao *et al.* (Figure 1) highlights the importance of monomer coordination in close proximity to the metal-O(polymer) chain, which may, in part, rationalise the reactivity enhancements observed with heterometallic **C1b-c**.[34] Catalysts **C1b** and **C1c** each feature a single initiating group per catalyst as an important feature. The lack of catalytic activity observed with homometallic **C2** and **C3** (Table 2) emphasizes the importance of initiating groups. Bimetallic catalysts with two initiating groups can produce two growing polymer chains;[35] in some cases, the two metal centres operate independently thus creating a misleading appearance of improved catalyst activity compared to the monometallic analogues. Further, close proximity between two propagating (metal-coordinated) polymer chains can result in enhanced chain transfer and transesterification, thus reducing polymerisation control.[74] Bimetallic catalysts with a single initiating group offer a means to improve control and reduce steric congestion around the metal centres, facilitating monomer access to key transition states involved in ROP.

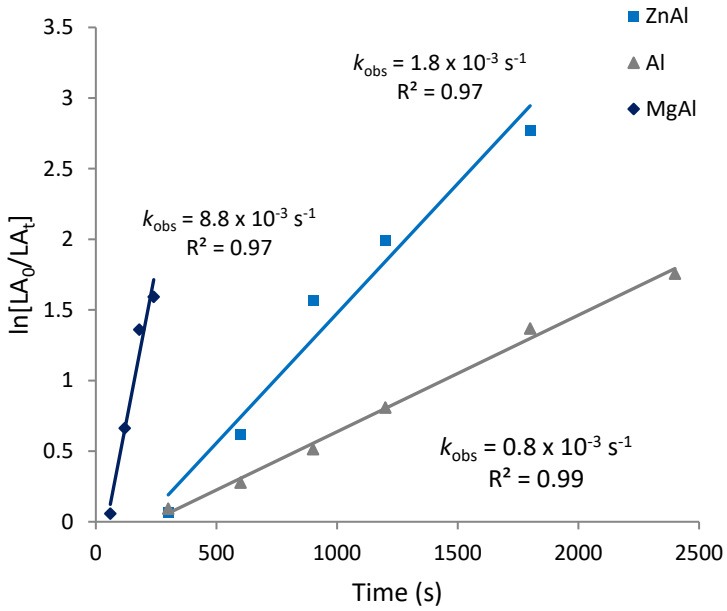

Figure 5 Kinetic plot of $\ln[LA]_0/\ln[LA]_t$ versus time for the ROP of *rac*-LA catalysed by complexes **C1b** (■), **C1c** (♦) and **C1** (▲). Reaction conditions: [catalyst]/[PO]/[*rac*-LA] = 1:50:100, [*rac*-LA] = 1 M in toluene, 120 °C.

Enhancing the metal Lewis acidity through salen ligand modification often improves propagation but reduces the initiation efficiency.[17,29,75] Heterometallic cooperativity may overcome this dichotomy: enhancing monomer coordination by providing additional Lewis acid sites, whilst also lengthening and weakening the Al-Cl bond to boost initiation. Heterometallic **C1b** and **C1c** outperform monometallic **C1** in both initiation efficiency and propagation rate. Computational modelling simulations performed on **C1** indicate that dynamic proton transfer occurs in the N_2O_2 pocket, with the optimised structure favouring the proton bound to the nitrogen atom. Elegant studies by Romain *et al.* on related (salen)Al complexes have shown that ligand N-H groups can facilitate LA coordination and activation through noncovalent interactions (NCIs).[76] However, with our bimetallic systems, tetra-deprotonated **C1b** and **C1c** outperform **C1** in LA

ROP, suggesting that any beneficial NCIs are outweighed by the Lewis acidic heterometal providing additional LA coordination sites or cooperative metal-metal effects, although the hindered accessibility of equatorial N-H groups in **C1** may also restrict LA coordination.[77]

The activity enhancements demonstrated by **C1b** and **C1c** correlate with literature reports showing that increased metal electropositivity can enhance LA polymerisation rate,[78] (Mg > Zn *vs* **C1**), whereas **C1a** (LiAl) and **C1d** (CaAl) contradict this trend. However, **C1a** and **C1d** both retain highly acidic phenolic protons, which may quench the polymerisation. Unlike conventional chain transfer agents, reactions with the phenolic protons would form resonance stabilised metal-phenoxide species as poor initiators, which may reduce the catalyst activity.

Extrapolation of the kinetic plots for catalysts **C1**, **C1b**, **C1a** and **C1c** gave polymerisation induction periods of 4 min, 3 min, 2.5 min and 1 min, respectively. Longer (and weaker) Al-Cl bonds (determined from the AIMD time-averaged structure) suggest a greater chloride nucleophilicity, which in turn drives a faster initiation step (Al-Cl bond lengths: **C1** 2.03 Å, **C1b** 2.22 Å, **C1a** 2.28 Å, **C1c** 2.30 Å, Table S3). Structures **C1b** and **C1c** suggest that magnesium acts as a better Cl lone pair electron acceptor than zinc, as evidenced by a shorter M-Cl bond length and reduced intermetallic separation (Figure 4 and Table 1). The longer Al-Cl bond in **C1c** may also indicate some "ate" behaviour, where the more electronegative metal (Zn > Al > Mg, *vide supra*) can adopt a formal negative charge, stabilised by the counter-cation formed from the electropositive metal.[36] For example, heterobimetallic combinations of metal halides $AlCl_3$, $MgCl_2$ and ZnF_2 have been shown to form aluminium zincates and magnesium aluminates through halide transfer to generate an ion pair.[79,80] Complexes **C1b** and **C1c** may therefore display some aluminium zincate and magnesium aluminate character, each containing a bridging halide due to

intermetal proximity. The formation of ate species could partially account for the improved reactivity of **C1c** and **C1b** by increasing the Lewis acidity of Mg/Al, as well as enhancing the nucleophilicity of the Al-OR/Zn-OR bond, respectively; monomer coordination and nucleophilic attack are both key steps in *rac*-LA ROP. A limited number of Al-Cl complexes have been reported for LA ROP, and the examples reported to date require an external or internal Lewis base (e.g. PPNCl[81] or electron donating ligand substituents) to increase the nucleophilicity of the Al-Cl bond towards initiation.[28] The use of onium salts such as PPNCl have been proposed to transfer a chloride ion to the Al metal centre to form an active aluminate species. Here, incorporation of a second Lewis acidic metal may mimic this effect, not only forming an active ate complex but providing the secondary benefit of additional metal coordination sites for monomer activation.

The introduction of divalent metals and consequent chloride bridging causes a distortion to square pyramidal geometry at the adjacent Al metal centre, correlating with increased ROP rates (Figure S62). Square pyramidal geometry provides a larger vacant site at Al relative to a trigonal bipyramidal coordination; an effect highlighted by comparing the Spacefill model of **C1c-I** (Gaussian calculations, $\tau5 = < 0.01$) to **C1a-II** (Gaussian calculations, $\tau5 = 0.83$) (Table 1, Figure S61). The vacant site provides an accessible surface for epoxide coordination during initiation and lactide coordination during propagation, thus avoiding long induction periods and low polymerisation activity. The tetra-anionic ligand scaffold prevents coordinative saturation at the metal centres, as only one co-ligand (initiator) is required for charge balance.[82] Studies on monometallic catalysts for cyclic ester ROP have suggested that trigonal bipyramidal geometries require lower framework distortion energies to access key octahedral transition states compared to the square pyramidal analogues; this reactivity trend appears to be less relevant or completely reversed with heterometallic complexes **C1b-c**.[83–85]

Within monometallic Al-salen complexes, increased ligand flexibility is generally accepted to improve cyclic ester polymerisation rates; this observation has been borne out by multiple experimental and computational studies.[28,29,84,85] Molecular dynamic DFT calculations can provide deeper insight into this key aspect of polymerisation catalysis. In contrast to monometallic literature systems, AIMD studies show that for heterobimetallic systems, reduced structural mobility (**C1c** << **C1b** < **C1a** < **C1**) generally corresponds to increased polymerisation rate (**C1c** > **C1b** > **C1** > **C1a**). Similarly, the ligand strain DFT calculations suggest that increased strain correlates with an increased rate of polymerisation (**C1c-I**: 197.2 kJ mol^{-1}, k_{obs} = 8.8 x 10^{-3} s^{-1} > **C1b-I**: 188.0 kJ mol^{-1}, k_{obs} = 1.8 x 10^{-3} s^{-1} > **C1a-I**: 159.9 kJ mol^{-1}, k_{obs} = 0.8 x 10^{-3} s^{-1}) (Table 1). With complexes **C1b** and **C1c**, the proximity of the heterometallic coordination site appears to overcome the need for ligand flexibility. Indeed, the increased strain in **C1b** and **C1c** may facilitate access to octahedral transition states previously proposed in cyclic ester ROP.[83] In contrast to monometallic salen systems,[84] our observations suggest that square pyramidal Al geometry facilitates monomer-metal coordination, and hence rapid polymerisation.

These observations suggest that the conventional design parameters established for monometallic (salen)Al ROP catalysts should be revisited for heterometallic analogues, which offer a promising method of improving catalyst performance. These studies also highlight the opportunity to use AIMD calculations within future catalyst development, showcasing the power of this method to capture time-averaged catalyst geometries and gain a deeper understanding of structure-activity relationships and the origins of heterobimetallic cooperativity. These insights provide underpinning methodologies for future heterometallic ROP catalyst design, which may also apply to other catalytic transformations, as aluminium salen catalysts have wide-reaching applications spanning small molecule transformations and ring-opening (co)polymerisation.

Conclusion

A series of mono- and bi-metallic complexes were derived from an acid salen ligand scaffold, characterised and tested for *rac*-LA ROP. The heterobimetallic MgAl and ZnAl catalysts significantly outperform the analogous monometallic Al complex, whereas the LiAl and CaAl catalysts do not. These studies emphasize that the heterometal must be carefully chosen as ionic radius, charge and electronegativity can all affect the complex structure and polymerisation activity. Previous studies with monometallic (salen)Al catalysts have shown that increased ligand flexibility improves catalyst activities in cyclic ester ROP, yet our studies show that this conventional wisdom does not hold true for heterometallic systems. Indeed, molecular dynamic simulations suggest that rigidity can be an important characteristic in heterobimetallic salen systems. This works unveils the potential of AIMD simulations in polymerisation catalysis, to understand structural flexibility and test experimental design methodology, leading to a deeper understanding of which catalyst features influence activity. Future heterometallic catalyst design should consider the introduction of a secondary metal as a promising method to simultaneously increase Lewis acidity and M-OR nucleophilicity as well as rigidity. These studies suggest that ROP catalyst design principles that are widely accepted for monometallic catalysts may need to be revisited for heterometallic systems, to exploit the exciting potential of cooperative heterometallic catalysis within cyclic ester ROP, as well as other fields.

AUTHOR INFORMATION

Corresponding Author

Corresponding author: Jennifer Garden

EaStCHEM School of Chemistry, University of Edinburgh, EH9 3FJ, UK

Email: j.garden@ed.ac.uk

Author Contributions

The manuscript was written through contributions of all authors. All authors have given approval to the final version of the manuscript.

Funding Sources

The authors gratefully acknowledge the University of Edinburgh, Royal Society (JAG, Grant RSG\R1\180101), L'Oréal-UNESCO for Women in Science Fellowship (JAG) and the British Ramsay Memorial Trust (JAG) for funding.

Acknowledgments

We acknowledge the University of Edinburgh ECDF and EaStCHEM Research Computing Facility for hardware and software access, respectively.

Abbreviations

AIMD, ab initio molecular dynamics; ADP, atomic displacement parameters; COSY, homonuclear correction spectroscopy; DFT, density functional theory; DMSO, dimethyl sulfoxide; ε-CL, ε-caprolactone; HMDS, bis(trimethylsilyl)amine; HSQC, heteronuclear single quantum correlation spectroscopy; ICP-OES, inductively coupled plasma optical emission spectrometry; LA, lactide; MALDI-ToF, matrix-assisted laser desorption/ionisation – time of flight; NCI, noncovalent interaction; PO, propylene oxide; PLA, poly(lactic acid); ROP, ring-opening polymerisation; RT, room temperature; TBP, trigonal bipyramidal.

References

1 J. Park and S. Hong, Cooperative Bimetallic Catalysts in Asymmetric Transformations, *Chem. Soc. Rev.*, 2012, **41**, 6931–6943.

2 A. J. Martínez-Martínez, A. R. Kennedy, R. E. Mulvey and C. T. O'Hara, Directed Ortho-Meta′- and Meta-Meta′-Dimetalations: A Template Base Approach to Deprotonation,

Science., 2014, **346**, 834–837.

3 T. D. Bluemke, W. Clegg, P. García-Alvarez, A. R. Kennedy, K. Koszinowski, M. D. McCall, L. Russo and E. Hevia, Structural and Reactivity Insights in Mg-Zn Hybrid Chemistry: Zn-I Exchange and Pd-Catalysed Cross-Coupling Applications of Aromatic Substrates, *Chem. Sci.*, 2014, **5**, 3552–3562.

4 S. Liu, A. Motta, A. R. Mouat, M. Delferro and T. J. Marks, Very Large Cooperative Effects in Heterobimetallic Titanium-Chromium Catalysts for Ethylene Polymerization / Copolymerization, *J. Am. Chem. Soc.*, 2014, **136**, 10460–10469.

5 S. K. Mandal, P. M. Gurubasavaraj, H. W. Roesky, G. Schwab, D. Stalke, R. B. Oswald and V. Dolle, Oxygen-Bridged Hybrid Metallocene-Nonmetallocene Polymetallic Catalysts of Group 4 Metals for Bimodal Activity in Olefin Polymerization: Synthesis, Characterization, and Theoretical Investigation, *Inorg. Chem.*, 2007, **46**, 10158–10167.

6 A. C. Deacy, E. Moreby, A. Phanopoulos and C. K. Williams, Co(III)/Alkali-Metal(I) Heterodinuclear Catalysts for the Ring-Opening Copolymerization of CO_2 and Propylene Oxide, *J. Am. Chem. Soc.*, 2020, **142**, 19150–19160.

7 A. C. Deacy, A. F. R. Kilpatrick, A. Regoutz and C. K. Williams, Understanding metal Synergy in Heterodinuclear Catalysts for the Copolymerization of CO_2 and Epoxides, *Nat. Chem.*, 2020, **12**, 372–380.

8 Z. Cai, D. Xiao and L. H. Do, Cooperative Heterobimetallic Catalysts in Coordination Insertion Polymerization, *Comments Inorg. Chem.*, 2019, **39**, 27–50.

9 R. A. Collins, A. F. Russell and P. Mountford, Group 4 Metal Complexes for Homogeneous Olefin Polymerisation: A Short Tutorial Review, *Appl. Petrochemical Res.*, 2015, **5**, 153–171.

10 H. Li and T. J. Marks, Nuclearity and Proximity Effects in Binuclear Catalysts and Cocatalysts for Olefin Polymerization, *Proc. Natl. Acad. Sci. U. S. A.*, 2006, **103**, 15295–15302.

11 M. Ainooson and F. Meyer, in *Comprehensive Inorganic Chemistry II (Second Edition): From Elements to Applications.*, Elsevier Ltd, 2013, **8**, 433–458.

12 R. G. Sinclair, The Case for Polylactic Acid as a Commodity Packaging Plastic, *J. Macromol. Sci. - Pure Appl. Chem.*, 1996, **33**, 585–597.

13 U. Edlund and A. C. Albertsson, Degradable Aliphatic Polyesters, *Adv. Polym. Sci.*, 2002, **157**, 67–112.

14 K. E. Uhrich, S. M. Cannizzaro, R. S. Langer and K. M. Shakesheff, Polymeric Systems for Controlled Drug Release, *Chem. Rev.*, 1999, **99**, 3181–3198.

15 M. Jamshidian, E. A. Tehrany, M. Imran, M. Jacquot and S. Desobry, Polylactic Acid: Production, Applications, Nanocomposites and Release Studies, *Compr. Rev. Food Sci. Food Saf.*, 2010, **9**, 552–571.

16 K. Hamad, M. Kaseem, H. W. Yang, F. Deri and Y. G. Ko, Properties and Medical Applications of Polylactic Acid: A Review, *Express Polym. Lett.*, 2015, **9**, 435–455.

17 M. J. Stanford and A. P. Dove, Stereocontrolled Ring-Opening Polymerisation of Lactide, *Chem. Soc. Rev.*, 2010, **39**, 486–494.

18 T. M. Ovitt and G. W. Coates, Stereoselective Ring-Opening Polymerization of Lactide with a Single Site, Racemic, Aluminium Alkoxide Catalyst: Synthesis of Stereoblock Poly(Lactic Acid), *J. Polym. Sci. Part A Polym. Chem.*, 2000, **38**, 4686–4692.

19 T. M. Ovitt and G. W. Coates, Stereochemistry of Lactide Polymerization with Chiral Catalysts: New Opportunities for Stereocontrol Using Polymer Exchange Mechanisms, *J. Am. Chem. Soc.*, 2002, **124**, 1316–1326.

20 Z. Zhong, P. J. Dijkstra and J. Feijen, [(Salen)Al]-Mediated, Controlled and Stereoselective Ring-Opening Polymerization of Lactide in Solution and Without Solvent: Synthesis of Highly Isotactic Polylactide Stereocopolymers from Racemic $_{D,L}$-Lactide, *Angew. Chemie - Int. Ed.*, 2002, **41**, 4510–4513.

21 N. Nomura, R. Ishii, M. Akakura and K. Aoi, Stereoselective Ring-Opening Polymerization of Racemic Lactide using Aluminium-Achiral Ligand Complexes: Exploration of a Chain-End Controlled Mechanism, *J. Am. Chem. Soc.*, 2002, **124**, 5938–5939.

22 N. Nomura, R. Ishii, Y. Yamamoto and T. Kondo, Stereoselective Ring-Opening Polymerization of a Racemic Lactide by Using Achiral Salen- and Homosalen-Aluminium Complexes, *Chem. - A Eur. J.*, 2007, **13**, 4433–4451.

23 A. Gualandi, F. Calogero, S. Potenti and P. G. Cozzi, Al(Salen) Metal Complexes in Stereoselective Catalysis, *Molecules.*, 2019, 24, 1716.

24 Y. A. Rulev, Z. Gugkaeva, V. I. Maleev, M. North and Y. N. Belokon, Robust Bifunctional Aluminium-Salen Catalysts for the Preparation of Cyclic Carbonates From Carbon Dioxide and Epoxides, *Beilstein J. Org. Chem.*, 2015, **11**, 1614–1623.

25 M. North, S. C. Z. Quek, N. E. Pridmore, A. C. Whitwood and X. Wu, Aluminum(Salen) Complexes as Catalysts for the Kinetic Resolution of Terminal Epoxides *via* CO_2 Coupling, *ACS Catal.*, 2015, **5**, 3398–3402.

26 A. Gualandi, M. Marchini, L. Mengozzi, H. T. Kidanu, A. Franc, P. Ceroni and P. G. Cozzi, Aluminum(III) Salen Complexes as Active Photoredox Catalysts, *European J. Org. Chem.*, 2020, **2020**, 1486–1490.

27 D. J. Darensbourg and D. B. Billodeaux, Aluminum Salen Complexes and Tetrabutylammonium Salts: A Binary Catalytic System for Production of Polycarbonates From CO_2 and Cyclohexene Oxide, *Inorg. Chem.*, 2005, **44**, 1433–1442.

28 A. J. Gaston, G. Navickaite, G. S. Nichol, M. P. Shaver and J. A. Garden, Electron Rich Salen-AlCl Catalysts as Efficient Initiators for the Ring-Opening Polymerisation of Rac-Lactide, *Eur. Polym. J.*, 2019, **119**, 507–513.

29 P. Hormnirun, E. L. Marshall, V. C. Gibson, R. I. Pugh and A. J. P. White, Study of Ligand Substituent Effects on the Rate and Stereoselectivity of Lactide Polymerization Using Aluminium Salen-Type Initiators, *Proc. Natl. Acad. Sci. U. S. A.*, 2006, **103**, 15343–15348.

30 A. Thevenon, C. Romain, M. S. Bennington, A. J. P. White, H. J. Davidson, S. Brooker and C. K. Williams, Dizinc Lactide Polymerization Catalysts: Hyperactivity by Control of Ligand Conformation and Metallic Cooperativity, *Angew. Chemie - Int. Ed.*, 2016, **55**, 8680–8685.

31 C. K. Williams, L. E. Breyfogle, S. K. Choi, W. Nam, V. G. Young, M. A. Hillmyer and W. B. Tolman, A Highly Active Zinc Complex for the Controlled Polymerization of Lactide, *J. Am. Chem. Soc.*, 2003, **125**, 11350–11359.

32 W. Gruszka, L. C. Walker, M. P. Shaver and J. A. Garden, In Situ Versus Isolated Zinc Catalysts in the Selective Synthesis of Homo- and Multi-block Polyesters, *Macromolecules.*, 2020, **53**, 4294–4302.

33 O. V. Kazarina, C. Gourlaouen, L. Karmazin, A. G. Morozov, I. L. Fedushkin and S. Dagorne, *Dalton Trans.*, 2018, **47**, 13800–13808.

34 L. Chen, W. Li, D. Yuan, Y. Zhang, Q. Shen and Y. Yao, Syntheses of Mononuclear and Dinuclear Aluminium Complexes Stabilized by Phenolato Ligands and Their Applications in the Polymerization of ε-Caprolactone: A Comparative Study, *Inorg. Chem.*, 2015, **54**, 4699–4708.

35 F. Isnard, M. Lamberti, L. Lettieri, I. D'Auria, K. Press, R. Troiano and M. Mazzeo, Bimetallic Salen Aluminium Complexes: Cooperation Between Reactive Centres in the Ring-Opening Polymerization of Lactide and Epoxides, *Dalton Trans.*, 2016, **45**, 16001–16010.

36 R. E. Mulvey, F. Mongin, M. Uchiyama and Y. Kondo, Deprotonative Metallation Using Ate Compounds: Synergy, Synthesis and Structure Building, *Angew. Chemie - Int. Ed.*, 2007, **46**, 3802–3824.

37 J. A. Garden, P. K. Saini and C. K. Williams, Greater Than the Sum of its Parts: A Heterodinuclear Polymerization Catalyst, *J. Am. Chem. Soc.*, 2015, **137**, 15078–15081.

38 G. Xiao, B. Yan, R. Ma, W. J. Jin, X. Q. Lü, L. Q. Ding, C. Zeng, L. L. Chen and F. Bao, Bulk Ring-Opening Polymerization (ROP) of L-Lactide Catalysed by Ni(II) and Ni(II)-Sm(III) Complexes Based on a Salen-Type Schiff Base Ligand, *Polym. Chem.*, 2011, **2**, 659–664.

39 L. L. Chen, L. Q. Ding, C. Zeng, Y. Long, X. Q. Lü, J. R. Song, D. Di Fan and W. J. Jin, Bulk Solvent-Free Melt Ring-Opening Polymerization of Lactide Catalysed by Cu(II) and Cu(II)-Nd(III) Complexes of the Salen-Type Schiff-Base Ligand, *Appl. Organomet. Chem.*, 2011, **25**, 310–316.

40 W. J. Jin, L. Q. Ding, Z. Chu, L. L. Chen, X. Q. Lü, X. Y. Zheng, J. R. Song and D. Di Fan, Controllable Bulk Solvent-Free Melt Ring-Opening Polymerization (ROP) of L-Lactide Catalysed by Ni(II) and Ni(II)-Ln(III) Complexes Based on the Salen-Type Schiff-Base Ligand, *J. Mol. Catal. A Chem.*, 2011, **337**, 25–32.

41 F. Hild, P. Haquette, L. Brelot and S. Dagorne, Synthesis and Structural Characterization of Well-Defined Anionic Aluminium Alkoxide Complexes Supported by NON-Type Diamido Ether Tridentate Ligands and Their use for the Controlled ROP of Lactide, *Dalton Trans.*, 2010, **39**, 533–540.

42 M. T. Muñoz, T. Cuenca and M. E. G. Mosquera, Heterometallic Aluminates: Alkali Metals Trapped by an Aluminium Aryloxide Claw, *Dalton Trans.*, 2014, **43**, 14377–14385.

43 J. Hao, J. Li, C. Cui and H. W. Roesky, Synthesis and Characterization of Heterobimetallic Oxo-Bridged Aluminum-Rare Earth Metal Complexes, *Inorg. Chem.*, 2011, **50**, 7453–7459.

44 A. H. Gao, W. Yao, Y. Mu, W. Gao, M. T. Sun and Q. Su, Heterobimetallic Aluminium and Zinc Complex with N-Arylanilido-imine Ligand: Synthesis, Structure and Catalytic Properties for Ring-Opening Polymerization of ε-Caprolactone, *Polyhedron.*, 2009, **28**, 2605–2610.

45 C. Jian, J. Zhang, Z. Dai, Y. Gao, N. Tang and J. Wu, Synthesis and Characterization of Magnesium Alkoxides Incorporated into Bulky Aluminium Tetraphenolate Helices and Application in the Ring-Opening Polymerization of Lactides, *Eur. J. Inorg. Chem.*, 2013, **2013**, 3533–3541.

46 B. M. Chamberlain, M. Cheng, D. R. Moore, T. M. Ovitt, E. B. Lobkovsky and G. W. Coates, Polymerization of Lactide with Zinc and Magnesium β-Diiminate Complexes: Stereocontrol and Mechanism, *J. Am. Chem. Soc.*, 2001, **123**, 3229–3238.

47 C. K. Williams, N. R. Brooks, M. A. Hillmyer and W. B. Tolman, Metalloenzyme Inspired Dizinc Catalyst for the Polymerization of Lactide, *Chem. Commun.*, 2002, **2**, 2132–2133.

48 F. Drouin, P. O. Oguadinma, T. J. J. Whitehorne, R. E. Prudhomme and F. Schaper, Lactide Polymerization with Chiral β-Diketiminate Zinc Complexes, *Organometallics.*, 2010, **29**, 2139–2147.

49 A. Garcés, L. F. Sánchez-Barba, J. Fernández-Baeza, A. Otero, M. Honrado, A. Lara-Sánchez and A. M. Rodríguez, Heteroscorpionate Magnesium Alkyls Bearing Unprecedented Apical σ-C(sp^3)-Mg Bonds: Heteroselective Ring-Opening Polymerization of R*ac*-Lactide, *Inorg. Chem.*, 2013, **52**, 12691–12701.

50 P. Bag, S. Dutta, U. Flörke and K. Nag, Solid State and Solution Properties of Lanthanide(III) Complexes of a Tetraiminodiphenolate Macrocyclic Ligand. X-Ray Structure, ^{1}H NMR and Luminescence Spectral Studies, *J. Mol. Struct.*, 2008, **891**, 408–419.

51 P. Bag, S. K. Maji, P. Biswas, U. Flörke and K. Nag, Macrocyclic Lanthanide(III) Complexes of Iminophenol Schiff Bases and Carboxylate Anions: Syntheses, Structures and Luminescence Properties, *Polyhedron.*, 2013, **52**, 976–985.

52 D. R. Lide, *CRC Handbook of Chemistry and Physics, 86th Edition.*, American Chemical Society (ACS), 2006.

53 K. P. Kepp, A Quantitative Scale of Oxophilicity and Thiophilicity, *Inorg. Chem.*, 2016, **55**, 9461–9470.

54 R. G. Pearson, Absolute Electronegativity and Hardness: Application to Inorganic Chemistry, *Inorg. Chem.*, 1988, **27**, 734–740.

55 A. F. Wells, *Structural Inorganic Chemistry*, Oxford [Oxfordshire] Clarendon Press, 5th ed., 1984.

56 R. D. Shannon, Revised Effective Ionic Radii and Systematic Studies of Interatomic Distances in Halides and Chalcogenides, *Acta Crystallogr. Sect. A.*, 1976, **32**, 751–767.

57 I. Morgenstern-Badarau, M. Rerat, O. Kahn, J. Jaud and J. Galy, Crystal Structure and Magnetic and EPR Properties of the Heterobinuclear Complex $CuNi(fsa)_2en(H_2O)_2.H_2O$ ($H_4(fsa)_2en$ = N,N'-bis(2-hydroxy-3-carboxybenzylidene)-1,2,-diaminoethane), *Inorg. Chem.*, 1982, **21**, 3050-3059.

58 M M. Mikuriya, H. Okawa, S. Kida and I. Ueda, Binuclear Metal Complexes, XXIII. Molecular Structure of a Heterometal Binuclear Complex, $CuCo(fsaen)\cdot 3H_2O(C_{18}H_{18}N_2O_9CoCu)$, *Bull. Chem. Soc. Jpn.*, 1978, **51**, 2920–2923.

59 A. Lalehzari, J. Desper and C. J. Levy, Double-Stranded Monohelical Complexes From an Unsymmetrical Chiral Schiff-Base Ligand, *Inorg. Chem.*, 2008, **47**, 1120–1126.

60 A. B. Kremer and P. Mehrkhodavandi, Dinuclear Catalysts for the Ring Opening Polymerization of Lactide, *Coord. Chem. Rev.*, 2019, **380**, 35–57.

61 M. Westerhausen, S. Schneiderbauer, A. N. Kneifel, Y. Söltl, P. Mayer, H. Nöth, Z. Zhong,

P. J. Dijkstra and J. Feijen, Organocalcium Compounds with Catalytic Activity for the Ring-Opening Polymerization of Lactones, *Eur. J. Inorg. Chem.*, 2003, **2003**, 3432–3439.

62 A. C. Deacy, C. B. Durr, J. A. Garden, A. J. P. White and C. K. Williams, Groups 1, 2 and Zn(II) Heterodinuclear Catalysts for Epoxide/CO_2 Ring-Opening Copolymerization, *Inorg. Chem.*, 2018, **57**, 15575–15583.

63 A. Rae, A. J. Gaston, Z. Greindl and J. A. Garden, Electron Rich (Salen)AlCl Catalysts for Lactide Polymerisation: Investigation of the Influence of Regioisomers on the Rate and Initiation Efficiency, *Eur. Polym. J.*, 2020, **138**, 109917-109921.

64 A. W. Addison, T. N. Rao, J. Reedijk, J. Van Rijn and G. C. Verschoor, Synthesis, Structure, and Spectroscopic Properties Of Copper(II) Compounds Containing Nitrogen-Sulphur Donor Ligands; the Crystal and Molecular Structure of Aqua[1,7-bis(N-methylbenzimidazol-2′-yl)-2,6-dithiaheptane]copper(II) Perchlorate, *J. Chem. Soc. Dalton Trans.*, 1984, **0**, 1349–1356.

65 A. M. Reilly, D. A. Wann, C. A. Morrison and D. W. H. Rankin, Experimental Equilibrium Crystal Structures: Molecular Dynamics as a Probe for Atomic Probability Density Functions, *Chem. Phys. Lett.*, 2007, **448**, 61–64.

66 A. M. Reilly, S. Habershon, C. A. Morrison and D. W. H. Rankin, Simulating Thermal Motion in Crystalline Phase-I Ammonia, *J. Chem. Phys.*, 2010, **132**, 134511-134519.

67 A. Hermann, S. Hill, A. Metz, J. Heck, A. Hoffmann, L. Hartmann and S. Herres-Pawlis, Next Generation of Zinc Bisguanidine Polymerization Catalysts Towards Highly Crystalline, Biodegradable Polyesters, *Angew. Chemie - Int. Ed.*, 2020, **59**, 21778–21784.

68 L. A. Román-Ramírez, P. McKeown, C. Shah, J. Abraham, M. D. Jones and J. Wood, Chemical Degradation of End-of-Life Poly(lactic acid) into Methyl Lactate by a Zn(II) Complex, *Ind. Eng. Chem. Res.*, 2020, **59**, 11149–11156.

69 X. Pang, H. Du, X. Chen, X. Wang and X. Jing, Enolic Schiff Base Aluminum Complexes and Their Catalytic Stereoselective Polymerization of Racemic Lactide, *Chem. - A Eur. J.*, 2008, **14**, 3126–3136.

70 H. L. Chen, S. Dutta, P. Y. Huang and C. C. Lin, Preparation and Characterization of Aluminum Alkoxides Coordinated on Salen-Type Ligands: Highly Stereoselective Ring-Opening Polymerization of *rac*-Lactide, *Organometallics*, 2012, **31**, 2016–2025.

71 Z. Tang, X. Chen, Y. Yang, X. Pang, J. Sun, X. Zhang and X. Jing, Stereoselective Polymerization of rac-Lactide with a Bulky Aluminum/Schiff Base Complex, *J. Polym. Sci. Part A Polym. Chem.*, 2004, **42**, 5974–5982.

72 Z. Wen, D. Li, J. Qi, X. Chen, Y. Jiang, L. Chen, B. Gao, Y. Cui and Q. Duan, Effect of the phenyl ring substituent on stereoselectivity in the ring-opening polymerization of the rac-

lactide initiated by salen aluminum complexes, *Colloid Polym. Sci.*, 2015, **293**, 3449–3457.

73 J. Baran, A. Duda, A. Kowalski, R. Szymanski and S. Penczek, Intermolecular Chain Transfer to Polymer with Chain Scission: General Treatment and Determination of k_p/k_{tr} in $_{L,L}$-Lactide Polymerization, *Macromol. Rapid Commun.*, 1997, **18**, 325–333.

74 J. Bai, X. Xiao, Y. Zhang, J. Chao and X. Chen, β-Pyridylenolate Zinc Catalysts for the Ring-Opening Homo- and Copolymerization of ε-Caprolactone and Lactides, *Dalton Trans.*, 2017, **46**, 9846–9858.

75 N. Spassky, M. Wisniewski, C. Pluta and A. Le Borgne, Highly Stereoelective Polymerization of Rac-($_{D,L}$)-Lactide with a Chiral Schiff's Base/Aluminium Alkoxide Initiator, *Macromol. Chem. Phys.*, 1996, **197**, 2627–2637.

76 S. Gesslbauer, R. Savela, Y. Chen, A. J. P. White and C. Romain, Exploiting Noncovalent Interactions for Room Temperature Heteroselective Rac-Lactide Polymerization Using Aluminum Catalysts, *ACS Catal.*, 2019, **9**, 7912–7920.

77 R. I. Storer, C. Aciro and L. H. Jones, Squaramides: Physical Properties, Synthesis and Applications, *Chem. Soc. Rev*, 2011, **40**, 2330–2346.

78 D. Cheshmedzhieva, I. Angelova, S. Ilieva, G. S. Georgiev and B. Galabov, Initiation of Ring-Opening Polymerization of Lactide: the Effect of Metal Alkoxide Catalyst, *Comput. Theor. Chem.*, 2012, **995**, 8–16.

79 A. Dashti, K. Niediek, B. Werner and B. Neumüller, Difluorenylzink als Alkylierungsmittel zur Darstellung von Triorganometallanen der 13. Gruppe. Synthese und Kristallstruktur von [$GaFl_3$(THF)].Toluol (Fl = Fluorenyl) *Z. Anorg. Allg. Chem.*, 1997, **623**, 394–402.

80 P. Sobota, T. Pluzinski, J. Utko and T. Lis, Evidence for the Existence of the $[MgCl(THF)_5]^+$ Cation: Crystal Structures of $[MgCl(THF)_5][FeCl_4]^-$ THF and $[MgCl(THF)_5][AlCl_4]^-$THF, *Inorg. Chem.*, 1989, **28**, 2217–2219.

81 C. Robert, T. E. Schmid, V. Richard, P. Haquette, S. K. Raman, M. N. Rager, R. M. Gauvin, Y. Morin, X. Trivelli, V. Guérineau, I. Del Rosal, L. Maron and C. M. Thomas, Mechanistic Aspects of the Polymerization of Lactide Using a Highly Efficient Aluminum(III) Catalytic System, *J. Am. Chem. Soc.*, 2017, **139**, 6217–6225.

82 A. C. Deacy, C. B. Durr and C. K. Williams, Heterodinuclear Complexes Featuring Zn(II) and M = Al(III), Ga(III) or In(III) for Cyclohexene Oxide and CO_2 Copolymerisation, *Dalton Trans.*, 2019, **49**, 223–231.

83 J. A. Macaranas, A. M. Luke, M. Mandal, B. D. Neisen, D. J. Marell, C. J. Cramer and W. B. Tolman, Sterically Induced Ligand Framework Distortion Effects on Catalytic Cyclic Ester Polymerizations, *Inorg. Chem.*, 2018, **57**, 3451–3457.

84 D. E. Stasiw, M. Mandal, B. D. Neisen, L. A. Mitchell, C. J. Cramer and W. B. Tolman, Why so slow? Mechanistic Insights from Studies of a Poor Catalyst for Polymerization of ϵ-Caprolactone, *Inorg. Chem.*, 2017, **56**, 725–728.

85 E. E. Marlier, J. A. MacAranas, D. J. Marell, C. R. Dunbar, M. A. Johnson, Y. DePorre, M. O. Miranda, B. D. Neisen, C. J. Cramer, M. A. Hillmyer and W. B. Tolman, Mechanistic Studies of ε-Caprolactone Polymerization by (salen)AlOR Complexes and a Predictive Model for Cyclic Ester Polymerizations, *ACS Catal.*, 2016, **6**, 1215–1224.

Table of Contents

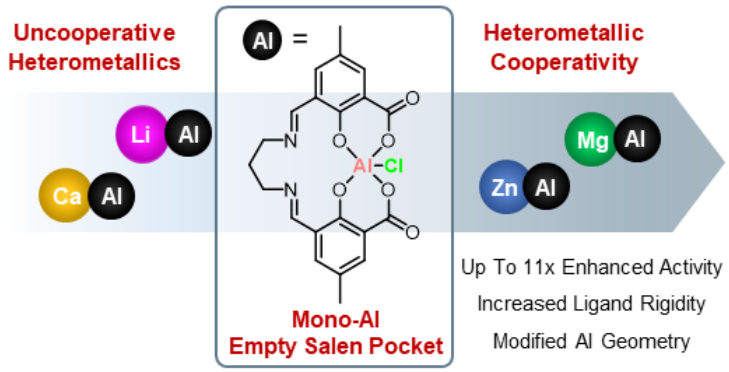

Synopsis:

Careful choice of the heterometal is key in determining whether or not heterometallic Al salen complexes exhibit cooperative catalysis in lactide ring-opening polymerisation. Experimental studies combined with ab initio molecular dynamic simulations reveal that metal-metal proximity, chloride bridging, aluminium centre geometry and ligand rigidity are important parameters underpinning cooperative catalysis, all of which are influenced by the heterometal.